Science of Sintering, **44** (2012) 25-33

Doi:10.2298/SOS1201025D

UDK 537.533.35:661.183.8

Mechanical Properties Correlation to Processing Parameters for Advanced Alumina Based Refractories

Marija M. Dimitrijević[1*)], Djordje Veljović[1], Milica Posarac-Marković[2], Radmila Jančić-Heinemann[1], Tatjana Volkov-Husović[1], Milorad Zrilić[1]

[1] University of Belgrade, Faculty of Technology and Metallurgy, 11000 Belgrade, Serbia

[2] University of Belgrade, Institute of Nuclear Sciences "Vinca", P.O. Box 522, 11001 Belgrade

Abstract:

Alumina based refractories are usually used in metallurgical furnaces and their thermal shock resistance is of great importance. In order to improve thermal shock resistance and mechanical properties of alumina based refractories short ceramic fibers were added to the material. SEM technique was used to compare the microstructure of specimens and the observed images gave the porosity and morphological characteristics of pores in the specimens. Standard compression test was used to determine the modulus of elasticity and compression strength. Results obtained from thermal shock testing and mechanical properties measurements were used to establish regression models that correlated specimen properties to process parameters.

Key words: *ceramics composites, image analysis, mechanical properties, electron microscopy*

1. Introduction

Alumina is the most cost effective and widely used material in the family of engineering ceramics. The raw materials from which this high performance technical grade ceramic is made are readily available and reasonably priced, resulting in good value for the cost in fabricated alumina shapes. With an excellent combination of properties and an attractive price, it is no surprise that fine grain technical grade alumina has a very wide range of applications [1].

Ceramic matrix composites (CMCs) combine reinforcing ceramic phases with a ceramic matrix to create materials with new and superior properties. In ceramic matrix composites, the primary goal of the ceramic reinforcement is to provide toughness to an otherwise brittle ceramic matrix. Chemical and thermal stability, relatively good strength, thermal and electrical insulation characteristics combined with availability in abundance have made aluminum oxide Al_2O_3, or alumina, attractive for engineering application [2].

Fiber reinforced composites (FRCs) have been greatly improved since the 1970s, and their use has been expanded rapidly in the world of civil engineering because of several advantages, such as, high strength, stiffness, ductility, and impact resistance. In the FRC, the spatial distribution, length, and orientation of the fiber inside the matrix can be used as a design variable, to optimize particular mechanical characteristics (stiffness, compliance,

*) **Corresponding author**: mdimitrijevic@tmf.bg.ac.rs,

weight, etc.) or particular response quantities (energy density, peak stress, displacements, etc.) of the composite. [3]

In fibre reinforced composites, strong and stiff fibers are usually embedded into a ductile matrix with the aim of enhancing mechanical properties, mainly strength, strength-to-weight ratio, etc. Under load, the matrix transmits the force to the fibers, which carry the most of applied load. The geometry and arrangement of fibers is also important in controlling the mechanical properties of a fiber reinforced composite.

Thermal shock resistance dictates refractory performance in many applications. In many instances, a twofold approach, i.e. (1) material properties [4-7] and/or (2) heat transfer conditions [8-10] is used to characterize thermal shock behavior of the refractories. As an alternative, information on the thermal shock behavior of refractories can be obtained experimentally.

2. Experimental procedure

2.1 Materials

Aluminum oxide is a very important ceramic which is extensively used as a high temperature, corrosion resistant refractory material. [11] Alumina based specimens were prepared using chamotte and clay as it was used in industrial production in Samot Arandjelovac. The fibers were ball milled for 1 h. Components were milling with Al_2O_3 balls in DI water in polyethylene bottle. Three series of samples were prepared. Samples were cylinders of dimensions 30 × 9 mm. One series consist of raw materials without the addition of alumina fibers, and other two series of samples were prepared using the addition of 1 wt.% and 2 wt.% of alumina fibers having the aspect ratio l/d ≈ 17). Two pressing forces, of 36 MPa and 50 MPa, were used for specimen compaction. The samples were sintered at 1200°C for 2h in oxidative atmosphere.

In this experiment Thermal Ceramics bulk fibers were used. Those fibers offer a maximum temperature range of between 1260º - 1549º C. They provide good chemical stability and resistance to chemical attack. The fibers were cracked in mortar. The goal of this operation was to obtain fibers having defined lengths to diameter ratios.

2.2 Mechanical characteristics

Mechanical characteristics were obtained using the standard compression test using the servo-hydraulic testing machine Instron 1332 with load cell of 100kN and 5kN with data acquisition system. Data for strengths and Young modulus were obtained from measured compression load and deformation. The morphology of the sintered samples was examined using a scanning electron microscope (SEM), Jeol JSM 5800, operated at 20 keV. The obtained SEM micrographs were analyzed using software for image analysis, Image Pro plus Program, version 4.0 for Windows. Porosity was obtained from SEM micrographs using image analysis techniques.

2.3 Thermal shock

Thermal stability of the refractories was determined experimentally by water quench test (ICS 81.080 SRPS B.D8.308 former JUS B. D8. 306). Samples were cylinders with 30.0 mm diameter and 9.0 mm high. In experimental procedure 12 samples were used and one sample was selected randomly from the set after 4, 8, 12 up to 16 cycles to be examined using ultrasonic measurements and image analysis. The samples were dried at 110°C and then

transferred into an electric furnace at 950°C and held for 40 min. The samples were then quenched into water and left for 3 min, dried and returned to the furnace at 950°C. This procedure was repeated until total destruction of sample or destruction of 50 and more percent of surface. The number of quenches to failure was taken as a measure of thermal shock resistance.

2.4 Image analysis

Image analysis was performed on samples after sintering and on samples exposed to defined number of quench experiments. The surface of the specimen was colored with blue chalk in order to enable determination of non-damaged and damaged surfaces. The images were treated using the Image Pro Plus program. [12] The program gives possibility to select parts of the image that are colored in a defined color and this was used to separate damaged and non-damaged surface. Simple visual inspection says that samples do not exhibit total destruction during test procedure until 16 cycles. Images of samples without fibers before and during testing are presented at the fig.1 Images of samples with 1 and 2 percent of fibers before and during testing are presented in fig.2 and fig.3.

In this study image analysis was used for the determination of surface damage level before and after a defined numbers of quenches. Sample's surfaces were marked by blue color in order to obtain better resolution and observe difference in damaged and none-damaged surfaces of the material. Results were given as ratio S (damage surface) and S_0 (surface before quenching) as function of number of quench experiments, N (Fig. 4).

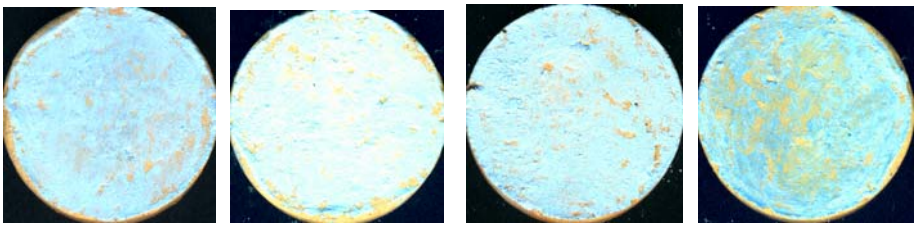

Fig. 1. Samples without fibres before and during testing

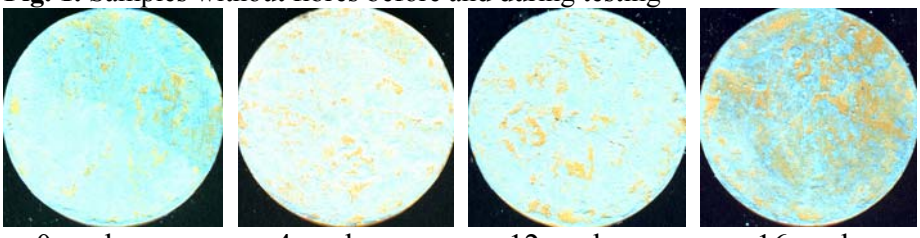

Fig. 2. Samples with 1% of fibers before and during testing

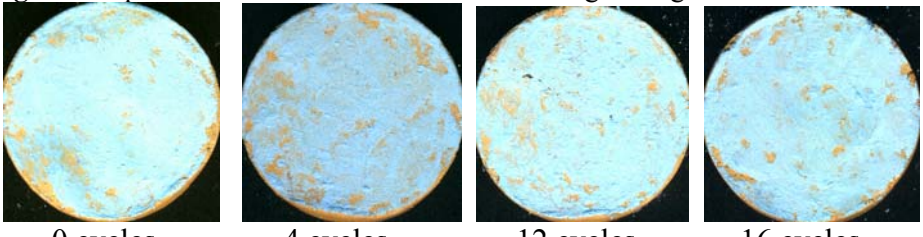

Fig. 3. Samples with 2 % of fibres before and during testing

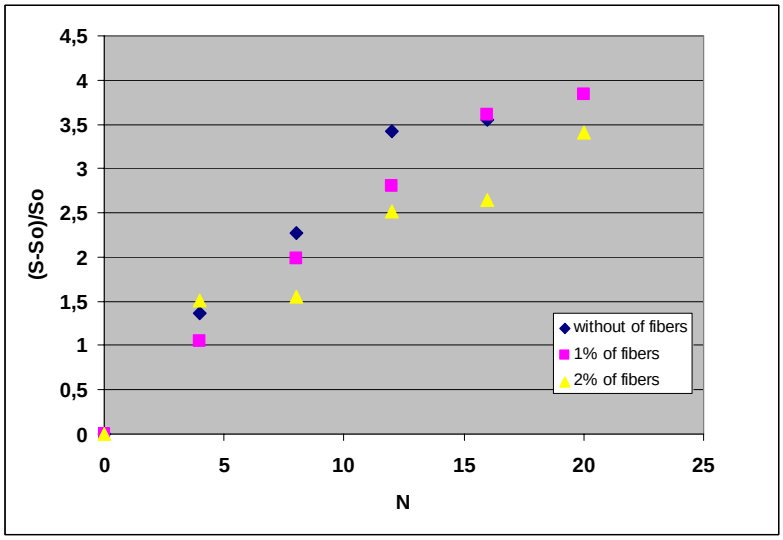

Fig. 4. Damage surface level (S) vs. number of quench experiments (N) fiber.

3. Results and discussion

Tab. I Compressive strengths of specimens having different fiber contents.

Samples	σ, MPa (compression) for preassure of 36 MPa	σ, MPa (compression) for preassure of 50 MPa
Without fibres	20,47	35,81
1% of fibres	33,88	39,11
2% of fibres	37,50	43,69

Short ceramic fibers were added to specimens in order to influence the crack propagation in them and to improve mechanical properties. The propagation of observed cracks was stopped by fibers and this could be seen in the micrographs, Fig. 5. On the other hand the measurements of modulus of elasticity gave results showing that the modulus of elasticity was decreased with addition of fibers into the composition.

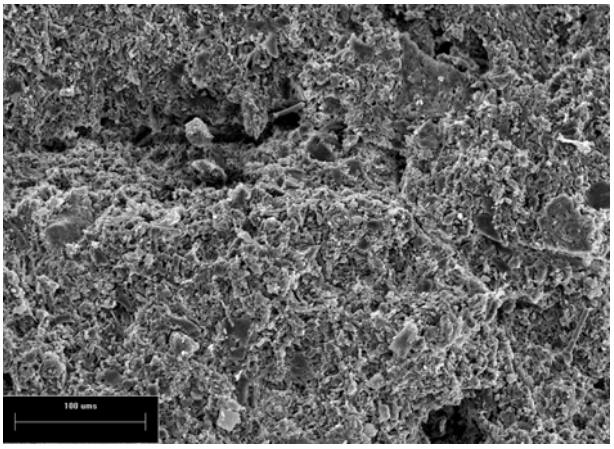

Fig. 5. SEM micrograph of the specimen pressed at 36MPa and having 1%volume of fibers showing the fiber in the specimen's structure that interacts with the crack and stoppes the crack propagation.

Several SEM images of every specimen were used to determine the porosity of specimens. The porosity was measured using the image analysis software. The method is based on the fact that the pores absorb more light and they appear darker in images compared to solid material [13]. The porosity increased with the addition of fibers and this could explain the decrease of bulk modulus of elasticity.

Strengths of specimens increase with addition of the fibers and increase with the pressure used for specimen compaction. Addition of fibers is advantageous for compressive strengths as is the increase of pressing force for specimen preparation.

Data of surface level damage, porosity, compressive strength and Young modulus of elasticity of samples were used for regression analysis. The data of the mathematical model are shown as a grid on the diagram and the points are the experimental data presented together with the model in order to illustrate the accordance of data to the regression model.

Surface degradation damage level was established as function of fiber content and number of cycles of thermal shock. The data concerning the pressure used for specimen preparation had much less statistical importance than those two parameters so this parameter was omitted from the model. Damage surface level of samples change according to the linear model:

$$\frac{\Delta S}{S_0} = 3.147 - 50.68x + 0.247N \quad (1)$$

Where : S_0 – damage surface level before exposure of the material to the thermal shock testing, x - the volume fraction of fibers, N - number of thermal shock cycles. The damage surface level increases with the number of cycles and decreases with the volume content of fiber. Squared correlation coefficient for this regression model is 0.81 and the graphical representation of data and regression dependence are shown in Fig. 6.

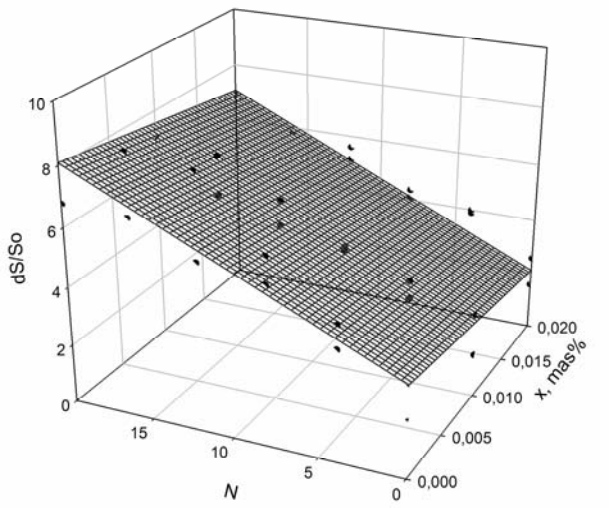

Fig. 6. Damage surface level of samples together with the regression dependence of trend data changes

Determining parameters for the compressive strength were the fiber content and the pressure used in compaction of specimens. Compressive strength of samples varies according to the linear model:

$$\sigma = 1.468 + 622.63x + 0.637P \quad (2)$$

Where x - the volume fraction of fibers added to the composition, and P – pressure used for compaction of specimens in MPa. The strength increases with increasing pressure and the fibers content showing that both parameters contribute to improvement of mechanical characteristics of the specimen. Squared correlation coefficient for this regression model is 0,880 and the graphical representation of data and regression dependence are given in Fig. 7.

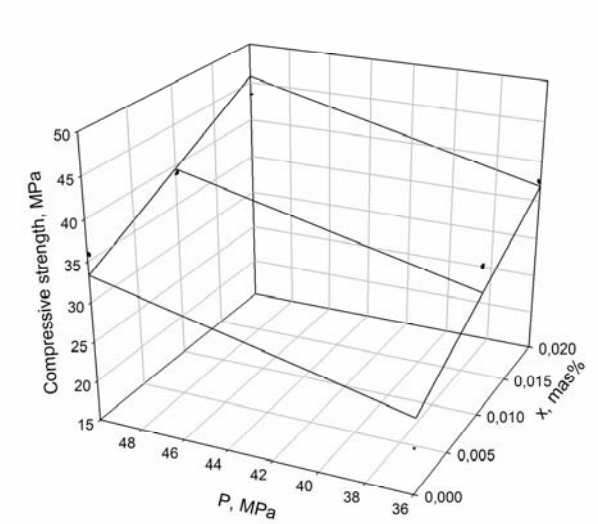

Fig. 7. Compressive strength of samples with regression dependence, which shows the trend of change data

Young modulus of elasticity was determined using the slope of the stress-strain curve obtained during the compressive test. It was found that Young modulus of elasticity is dependent on two parameters – volume fraction of fibers and pressure used for sample preparation. The linear regression model is given by equation (3):

$$E = 0.82 - 14.6x + 0.00149P \quad (3)$$

Where: x - the volume fraction of fibers added to the composition, and P - pressure. Young modulus increases with increasing pressure and decreases with increase in the fiber content. Squared correlation coefficient for this regression model is 0,977 and the graphical representation of data and regression the dependence shows Fig. 8.

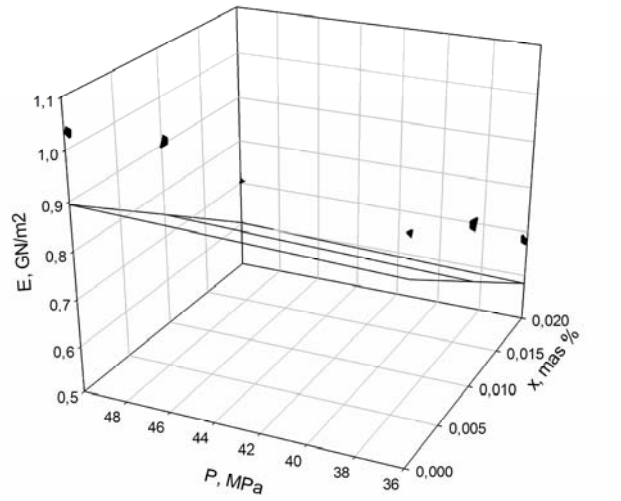

Fig. 8. Young modulus of elasticity of samples with regression dependence, which shows the trend of change data

Porosity of the specimens was determined from SEM images using image analysis as shown in Fig. 9.

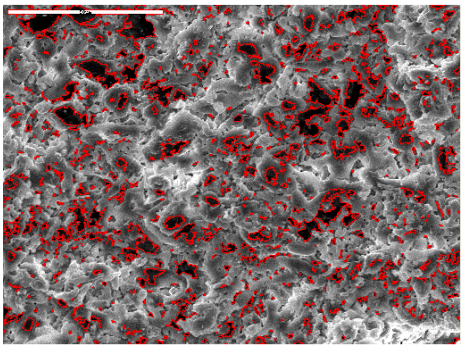

Fig. 9. Porosity of the specimens

Porosity of the sample varies according to the linear model:

$$Porosity = 10.895 + 76.5x - 0.0385P \quad (4)$$

Where: x - the volume fraction of fibers added to the composition, and P - pressure. Porosity of the samples increases with increase in the fiber content and decreases by increasing the pressure. Squared correlation coefficient for this regression model is 0,897 and the graphical representation of data and regression the dependence are given Fig. 10.

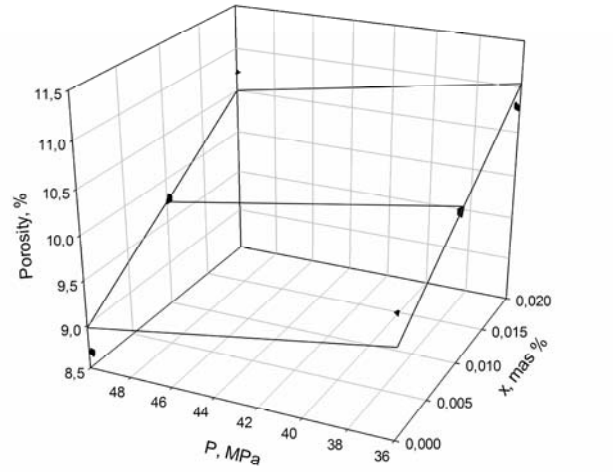

Fig. 10. Porosity of samples with regression dependence, which shows the trend of change data

Conclusion

Alumina based specimens strengths were improved using the addition of short ceramic fibers. This was also confirmed with observation of microstructure as the fibers stopped the crack propagation. This proved that the lengths to diameter ratio were well chosen. The decreases of modulus of elasticity correspond to increase in specimen porosity. The optimization of microstructure and properties could be done using the addition of fibers and changing the pressing force for specimen compaction. The content of fibers added is relatively limited as their addition could be cost effective.

Acknowledgements

This research has been financed by the Ministry of Science and Environment of the Republic of Serbia as a part of the projects TR34011, OI 142016, TR16004, III45019 and III 45012.

References

1. Pertti Auerkari, Mechanical and physical properties of engineering alumina ceramics, Technical Research Centre of Finland ESPOO 1996
2. http://accuratus.com/alumox.html
3. YunMook Lim, HongGyoo Sohn, GiHong Kim, SeungKyo Shin, Pang-jo Chun, Extraction of geometrical information for fiber pull-out using 3D image processing, Materials Letters 63 (2009) 645–648
4. D.P.H. Hasselman, Unified theory of thermal shock fracture initiation and crack propagation in brittle ceramics, J. Am. Ceram. Soc. 52 (1) (1969) 600–604.
5. D.P.H. Hasselman, Elastic energy at fracture and surface energy as design criteria for thermal shock, J. Am. Ceram. Soc. 46 (11) (1963) 535–540.
6. J. Nakayama, Direct measurements of fracture energies of brittle heterogenius materials, J. Am. Ceram. Soc. 48 (11) (1965) 583–587.
7. J. Nakayama, M. Ishizuka, Experimental evidence for thermal shock damage resistance, Am. Ceram. Soc. Bull. 45 (7) (1965) 666–669.
8. W.D. Kingery, Factors affecting thermal stress resistance of ceramic materials, J. Am. Ceram. Soc. 38 (1) (1955) 3–15.
9. S.S. Manson, R.W. Smith, Theory of thermal shock resistance of brittle materials based on Weibulls statistical theory of strength, J. Am. Ceram. Soc. 38 (1) (1955) 18–27.
10. H. Hencke, J.R. Thomas, D.P.H. Hasselman, Role of the material properties in the thermal-stress fracture of brittle ceramics subjected to the conductive heat transfer, J. Am. Ceram. Soc. 67 (6) (1984) 393–398.
11. R.F. Bunshah, Handbook of Hard Coatings, Noyes Publications, 2001.
12. Image Pro Plus, Reference Guide for Windows, 1993.
13. Rahul P. Talegaonkar and K. Gopinath, Influence of Alumina Fiber Content on Properties of Non-Asbestos Organic Brake Friction Material, Journal of Reinforced Plastics and Composites 2009 28: 2069 originally published online 27 June 2008
14. M.S. Djošić, V.B. Mišković-Stanković, Z.M. Kačarević-Popović, B.M. Jokić, N. Bibić, M. Mitrić, S.K. Milonjić, R. Jančić-Heinemann, J. Stojanović, Electrochemical synthesis of nanosized monetite powder and its electrophoretic deposition on titanium, Colloids and Surfaces A: Physicochem. Eng. Aspects 341 (2009) 110–117
15. Radmila Jancic, Radoslav Aleksic, Influence of formation conditions and precursor viscosity on mean fiber diameter formed using the rotating disk method, Materials Letters 42, (2000), 350–355
16. N.M. Talijan, A. Milutinovic-Nikolic, R. Jancic, I. Petrovic-Prelevic, J. Stajic-Trosic, The influence of the sintering regime on the stability of the $SmCo_5$ phase, Materials Letters 32 (1997) 85-89.
17. Boccaccini, D.N., Cannio, M., Volkov-Husovic, T.D., Kamseu, E., Romagnoli, M., Veronesi, P., Leonelli, C., Boccaccini, A.R., Service life prediction for refractory materials , Journal of Materials Science, ISSN 0022-2461 , 43 2008 (12), pp. 4079-4090

18. M. Posarac, M. Dimitrijavic, , T.Volkov Husovic J. Majstorovic, B. Matovic, The Ultrasonic and Image Analysis Method for Non-Desytuctove Mthod of Quantification of Thermal Shock Damage in Refractory Specimen, Materials and Design 30 (8), pp. 3338-3343,
19. S. Martinović, M. Vlahović, J. Majstorović, M.Dojcinović, and T. Volkov-Husović, Thermo-Mechanical Properties and Cavitation Resistance of High Alumina Low Cement Castable, Applied Ceramic Tecnology, ISSN 0350-820X, (2011), DOI:10.1111/j.1744-7402.2010.02545.x

Садржај: *Алуминозни ватростални материјали најчешће се користе у пећима у металуршком инжењерству где је од изузетне важности њихова термостабилност (отпорност на термошок). У циљу побољшавања термостабилности и механичких својстава ове групе материјала додавана су кратка керамичка влакна. Карактеризација микроструктуре узорака одређена је скенинг електронском микроскопијом (SEM), а резултати су коришћени ради поређења порозности и морфолошких карактеристика посматраних узорака. Коришћена је стандардна лабораторијска метода одређивања чврстоће и Јунговог модула еластичности. Добијени резултати везани за термостабилност и механичка својства послужила су за формирање модела који повезује својства узорка са процесним параметрима.*

Кључне речи: *керамички композит, анализа слике, механичка својства, електронска микроскопија*